NEOPLASIA
www.neoplasia.com

Volume 20 Number 12 December 2018 pp. 1209–1218 1209

The DEK Oncoprotein Functions in Ovarian Cancer Growth and Survival[1]

Kari E Hacker[*,2,3], Danielle E Bolland[*,2], Lijun Tan[*], Anjan K Saha[†], Yashar S Niknafs[‡], David M Markovitz[†] and Karen McLean[*]

[*]Division of Gynecologic Oncology, Department of Obstetrics and Gynecology, University of Michigan Medical Center, Ann Arbor, MI 48109; [†]Department of Internal Medicine and Cancer Biology Program, University of Michigan Medical Center, Ann Arbor, MI 48109; [‡]Michigan Center for Translational Pathology, University of Michigan Medical Center, Ann Arbor, MI 48109

Abstract

DNA damage repair alterations play a critical role in ovarian cancer tumorigenesis. Mechanistic drivers of the DNA damage response consequently present opportunities for therapeutic targeting. The chromatin-binding DEK oncoprotein functions in DNA double-strand break repair. We therefore sought to determine the role of DEK in epithelial ovarian cancer. DEK is overexpressed in both primary epithelial ovarian cancers and ovarian cancer cell lines. To assess the impact of DEK expression levels on cell growth, small interfering RNA and short hairpin RNA approaches were utilized. Decreasing DEK expression in ovarian cancer cell lines slows cell growth and induces apoptosis and DNA damage. The biologic effects of DEK depletion are enhanced with concurrent chemotherapy treatment. The *in vitro* effects of DEK knockdown are reproduced *in vivo*, as DEK depletion in a mouse xenograft model results in slower tumor growth and smaller tumors compared to tumors expressing DEK. These findings provide a compelling rationale to target the DEK oncoprotein and its pathways as a therapeutic strategy for treating epithelial ovarian cancer.

Neoplasia (2018) 20, 1209–1218

Introduction

Among women in the United States, ovarian cancer is the fifth highest cause of cancer-related deaths and is the deadliest gynecologic malignancy [1,2]. Standard initial therapy consists of surgical debulking and combination chemotherapy with a platinum and taxane-based regimen. Although the majority of ovarian cancers initially respond to treatment, almost all advanced-stage cancers recur and ultimately become resistant to platinum-based therapy. Five-year survival rates for patients diagnosed with epithelial ovarian cancer are approximately 50% [2].

A major hallmark of ovarian cancer is alterations in DNA damage repair pathways with resultant chromosomal aberrations, and over 50% of high-grade serous ovarian cancers (HGSOCs) display defective homologous recombination (HR) [3–5]. The Cancer Genome Atlas project has shown that the HR pathway is frequently mutated in HGSOC, with *BRCA1* and *BRCA2* gene mutations most common [3,5,6]. These mutations in the HR pathway are thought to contribute to platinum sensitivity in HGSOC, such that women with germline *BRCA* mutations demonstrate improved survival [3,7]. Although significant advances have been made in our understanding of the importance of DNA damage repair pathways in ovarian cancer,

Address all correspondence to: Karen McLean, MD, PhD, University of Michigan, 1500 E. Medical Center Drive, Ann Arbor, MI 48109-5276.
E-mail: karenmcl@umich.edu

[1] Funding: This work was supported in part by the Michigan Ovarian Cancer Alliance Geri Fournier Ovarian Cancer Research Awards to K. M., by R01 DK 109188 from the National Institutes of Health to D.M., and by the generous support of the Haller Family and the Goldberg Family.

[2] These authors contributed equally to this work.

[3] Present address: Gynecologic Oncology, New York University Langone Health, New York, NY.

Received 23 August 2018; Revised 11 October 2018; Accepted 16 October 2018

1476-5586
https://doi.org/10.1016/j.neo.2018.10.005

the development of resistance to current chemotherapies still remains the central challenge in the treatment of ovarian cancer. Therefore, additional therapeutic targets and biomarkers are necessary to improve treatment outcomes.

DEK is a highly conserved nuclear protein that binds chromatin and functions in multiple critical cellular processes, including DNA damage repair [8–11], RNA transcriptional regulation [12], mRNA splicing [13], and DNA replication [14]. Studies have also demonstrated that elevated DEK levels promote proliferation, motility, invasion [14], and tumorigenesis [15–18]. Further, DEK is crucial to global heterochromatin integrity [19]. In melanoma cell lines, shRNA-mediated DEK depletion resulted in cell cycle arrest and enhanced cellular senescence, as well as increased doxorubicin-induced cellular apoptosis [18]. Elevated DEK levels in breast cancer cell lines have been reported to correlate with disease recurrence and metastasis [14,20]. Given the critical role of DNA damage repair pathways in epithelial ovarian cancer and the reported roles of DEK in tumorigenesis and DNA repair, we sought to determine the role of DEK in ovarian cancer.

In this study, we demonstrate that DEK expression is elevated in a large panel of primary ovarian cancers as well as ovarian cancer cell lines. Decreasing DEK expression resulted in decreased proliferation, increased apoptosis, and increased DNA double-stranded breaks. These effects were enhanced with concurrent chemotherapy, suggesting a potential role for DEK in chemotherapy resistance. Finally, decreased DEK expression significantly slowed tumor growth in an *in vivo* xenograft model. Together, these results suggest that DEK may be a potential novel therapeutic target for the treatment of epithelial ovarian cancer.

Materials and Methods

Cell Culture and Drug Treatments

The human CAOV3 ovarian cancer cell line was maintained in Dulbecco's modified Eagle's medium supplemented with 10% fetal bovine serum. OVCAR8 and OVCAR3 human ovarian cancer cells were grown in RPMI medium supplemented with 10% fetal bovine serum. Human ovarian surface epithelial cells (HOSEpiC, ScienCell Research Laboratories) were cultured in ovarian epithelial cell medium supplemented with ovarian epithelial cell growth supplement per supplier instructions. All cell lines were incubated at 37°C in a 5% CO2 incubator. Cell lines were authenticated by STR profile testing in August 2016 or obtained in 2017 from ATCC or the National Cancer Institute. Cell lines were tested every 2 months for mycoplasma contamination (Invivogen). Pharmaceutical-grade chemotherapy agents or inhibitors were obtained from the University of Michigan Hospital Pharmacy: doxorubicin (Pfizer), cisplatin (Teva), and panobinostat (ApexBio). For each cell line and with each treatment studied, the IC50 was determined using the Biotium MTT Cell Proliferation Assay Kit (ThermoFisher).

Transient Transfection and Lentiviral Infection

For transient transfections, CAOV3 or OVCAR8 cells were grown to approximately 50% confluence and transfected using Lipofectamine 2000 (ThermoFisher) transfection reagent and 30 pmol of siRNA targeting DEK (Santa Cruz Biotechnology) or control siRNA (Santa Cruz Biotechnology). For lentiviral infections, constructs containing a short hairpin RNA targeting nucleotides 1165-1185 of DEK (shDEK1) or control nucleotides (shControl1) [18] were packaged into particles expressing the surface glycoprotein of vesicular stomatitis virus by the University of Michigan Vector Core Facility. Additional short hairpin RNA constructs for control (shControl2) or DEK were designed through Sigma-Aldrich targeting nucleotides 860-880 (shDEK2) and 1192-1216 (shDEK3). CAOV3, OVCAR8, or OVCAR3 cells were infected with the lentivirus with 8 μg/ml polybrene (Millipore). For stable expression of short hairpin RNAs, cell lines were infected with lentiviral constructs, and polyclonal lines were selected in puromycin (Sigma-Aldrich).

MTT Assay

CAOV3, OVCAR8, or OVCAR3 cells were plated in 96-well plates at a density of 5×10^3 cells per well. Cells were infected with lentiviral constructs targeting DEK or control nucleotides for 24 hours and subsequently treated for an additional 48 hours with the following drugs and concentrations based on IC50 determination for each cell line: cisplatin (CAOV3, 15 μM; OVCAR8, 25 μM; OVCAR3, 2 μM), doxorubicin (all cell lines, 200 nM), or panobinostat (CAOV3 and OVCAR8, 500 nM; OVCAR3, 200 nM). Cells were assessed for cell viability using the Biotium MTT Cell Proliferation Assay Kit (ThermoFisher). Briefly, cells were incubated at 37°C with the MTT solution [3-(4,5-dimethylthiazol-2-yl)-2,5-diphenyltetrazolium bromide] for 4 hours, and then the formazan salt was solubilized by the addition of dimethylsulfoxide. The absorbance values were read on a spectrophotometer at 570 nm and 630 nm for background reference. Samples were normalized to controls.

SDS-PAGE and Western Blots Analysis

Cultured cells were lysed in freshly made cold RIPA buffer (Sigma) containing protease (ThermoFisher) and phosphatase (Roche) inhibitor cocktail for 30 minutes. Protein concentrations were determined using the BCA Assay Kit (ThermoFisher). Equal amounts of proteins were separated on 4%-12% gradient NuPAGE SDS gel (Invitrogen) and transferred to a PVDF membrane (Millipore). Antibodies for immunoblotting included DEK (BD Biosciences), MCL-1 (Cell Signaling), cleaved caspase-3 (Cell Signaling), caspase-9 (Cell Signaling), phospho-histone γH2A.X (serine 139) clone JBW301 (Millipore), Rad51 (Calbiochem), and GAPDH (Cell Signaling). Bands were visualized using a commercial ECL kit (Pierce). The densitometry of each band was measured using ImageJ, and intensities were normalized to shControl with mock treatment.

Immunofluorescence

CAOV3, OVCAR8, or OVCAR3 cells (1×10^4 cells per chamber) were plated on chamber slides and incubated overnight. Cells were infected with shDEK1 or shControl1 lentivirus for 24 hours and then treated for an additional 24 hours with the following drugs: cisplatin (CAOV3, 15 μM; OVCAR8, 25 μM; OVCAR3, 2 μM), doxorubicin (all cell lines, 200 nM), or panobinostat (CAOV3 and OVCAR8, 500 nM; OVCAR3, 200 nM). Following treatment, cells were fixed with 4% paraformaldehyde, permeabilized with 0.5% Trition X-100, and stained with γH2A.X (Millipore) primary antibody and fluorescently labeled secondary antibody. Coverslips were mounted using Prolong Gold with DAPI (Thermofisher) for nuclear staining. Stained foci were visualized using Olympus IX83 fluorescent inverted microscope; representative images are shown.

The number of foci per cell was quantified using ImageJ with the following methodology. All cells that were entirely in the image were

subjected to focus counting. The absolute number of cells counted varied by cell line and treatment, with 2-18 cells counted for each condition. Foci were counted if they localized to the DAPI-positive portion of the cell, indicative of nuclear localization. To differentiate foci from background, easily distinguishable bright spots that were circular in morphology were identified, and the ImageJ multipoint tool was used to select individual foci and tally the total count per cell. All counted cells were included in statistical analysis.

Apoptosis

CAOV3, OVCAR8, or OVCAR3 cells were infected with shDEK or shControl lentivirus for 24 hours followed by treatment with the following drugs for an additional 48 hours: cisplatin (CAOV3, 15 μM; OVCAR8, 25 μM; OVCAR3, 2 μM), doxorubicin (all cell lines, 200 nM), or panobinostat (CAOV3 and OVCAR8, 500 nM; OVCAR3, 200 nM). Cells were stained for Annexin V-FITC and propidium iodide (BD Biosciences) and analyzed by flow cytometry. All flow cytometry analyses were performed at the University of Michigan Flow Cytometry Core. Caspase-3/7 activity was measured using the Caspase-Glo 3/7 assay (Promega). CAOV3, OVCAR3, or OVCAR8 cells were seeded in 96-well, white-walled plates (5×10^4 cells per well) and incubated overnight. Cells were infected with shDEK1 or shControl1 lentivirus for 24 hours. After infection, cells were treated for an additional 48 hours with cisplatin (CAOV3, 15 μM; OVCAR8, 25 μM; OVCAR3, 2 μM), doxorubicin (all cell lines, 200 nM), or panobinostat (CAOV3 and OVCAR8, 500 nM; OVCAR3, 200 nM). Caspase-Glo 3/7 detection reagent was added to each well and incubated at room temperature for 1 hour. Luminescence was measured using BioTek SYNERGY H1 plate reader. No-cell background luminescence was subtracted for all readings, and samples were normalized to shControls.

In Vivo Xenografts

All studies were performed with approval of the University Committee on Use and Care of Animals of the University of Michigan. Polyclonal CAVO3 cells (5×10^5 cells) cells stably expressing control shRNA or shRNA targeting DEK were injected subcutaneously into the bilateral axillae of 6-week-old female NOD-SCID mice (Charles River Breeding Labs) with growth factor–reduced Matrigel (BD Biosciences). One cohort of mice received cells with control shRNA bilaterally, and a second cohort received cells with shRNA targeting DEK bilaterally. Mice were monitored, and tumor volume was calculated using the modified ellipsoid equation ($L \times W \times W/2$, where L represents length and W represents width) until the tumor burden in one mouse in the cohort reached 2000 mm^3. All animals were then sacrificed, and tumors were measured and weighed. Five mice with bilateral axillary xenografts were used per group (n = 10 tumors).

Tissue Microarray and Immunohistochemistry

All studies were performed with the approval of the Institution Review Board of the University of Michigan. All samples were evaluated by a pathologist, and a morphologically representative region was selected from the hematoxylin–eosin staining. Tissue cores were collected from formalin-fixed, paraffin-embedded sections of primary ovarian tumor specimens (n = 91) and normal ovarian tissue

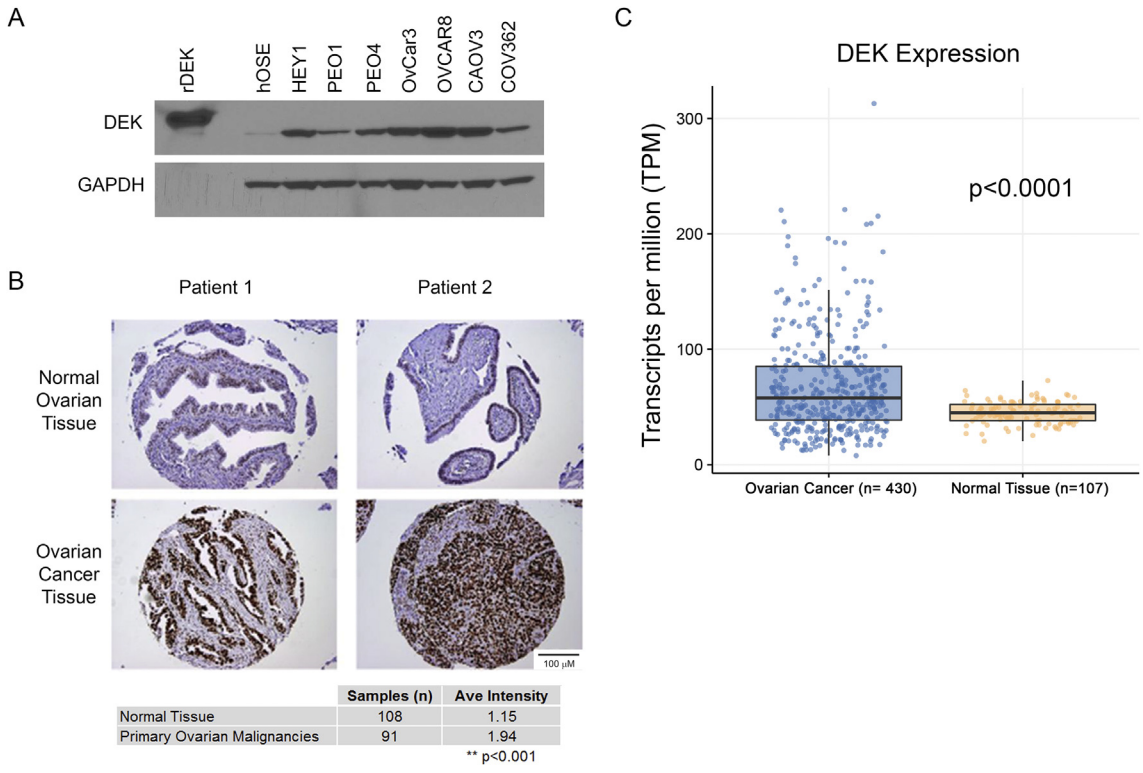

Figure 1. DEK is overexpressed in epithelial ovarian cancer cell lines and primary tumor specimens.(A) hOSE and a panel of human ovarian cancer cell lines were harvested, and samples containing equal amounts of protein were analyzed by immunoblotting for DEK expression. Recombinant DEK served as a positive control. GAPDH loading control is shown. (B) DEK immunohistochemistry was performed on a tissue microarray containing normal ovarian tissue and primary ovarian tumor specimens. Representative staining is shown. Tabulated findings and statistical results are indicated. (C) RNA-seq data processing of publically available database results reveals a statistically significant upregulation of DEK transcripts in ovarian cancer specimens as compared to normal ovary control tissues.

(108), as previously described [21]. For immunohistochemical analysis of both the TMA and *in vivo* xenograft tumors, formalin-fixed, paraffin-embedded sections were cut at 5 μm and rehydrated with water. Heat induced epitope retrieval was performed with FLEX TRS Low pH Retrieval buffer (pH 6.1) (Dako, North America) for 20 minutes. After blocking with peroxidase, the primary DEK mouse monoclonal antibody (BD Biosciences) was applied at a dilution of 1:400 at room temperature for 1 hour. The FLEX + Mouse EnVision System was used for detection. DAB chromagen was then applied. Slides were counterstained with Harris hematoxylin and then dehydrated, and coverslips were applied. All immunohistochemistry was performed at the University of Michigan Comprehensive Cancer Center Tissue Core. The tissue microarray was blindly scored on a scale of 0-3, with 0 indicating no expression and 3 indicating intense, diffuse staining. Staining between cancer and noncancer groups was compared using Student's *t* test.

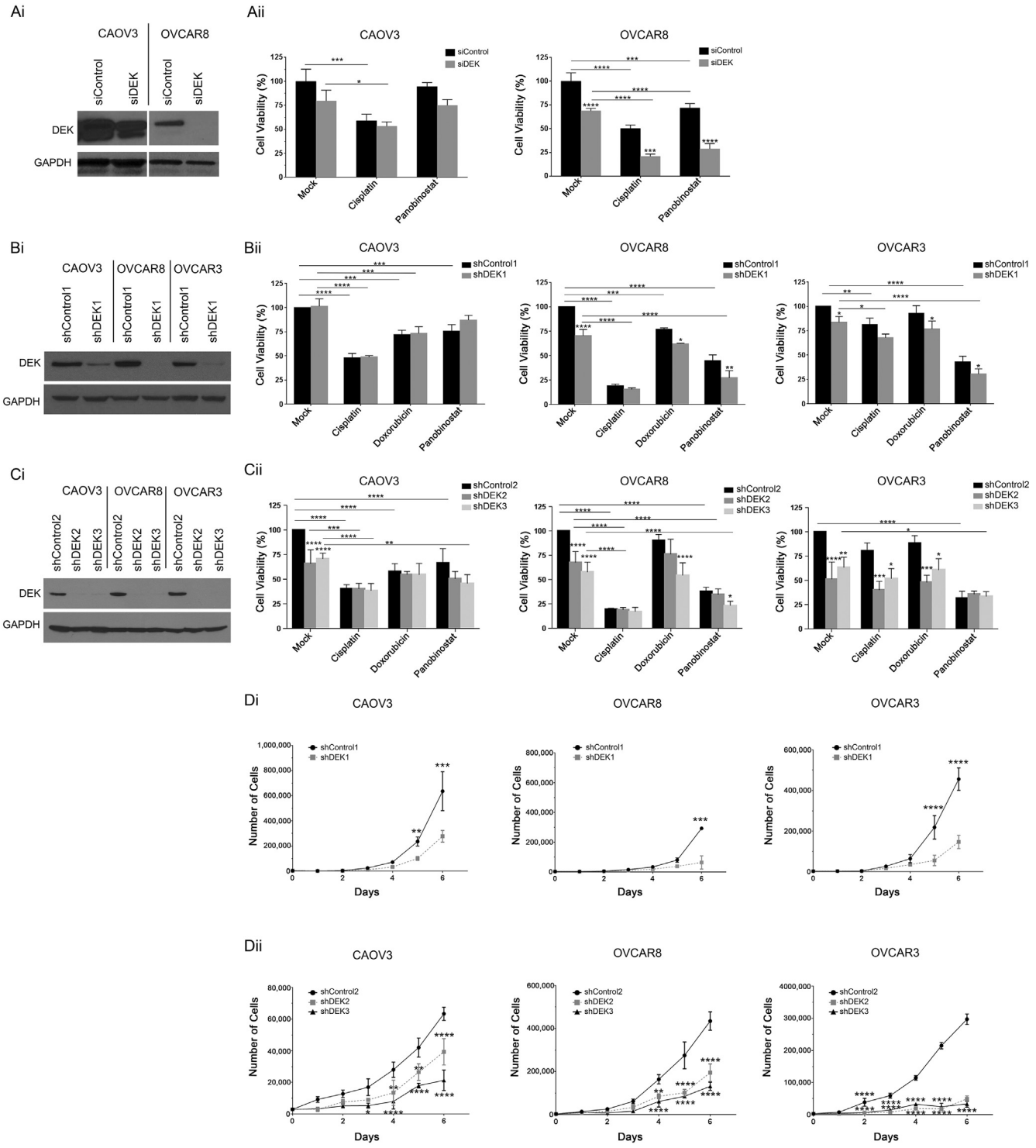

RNA-Sequencing Data Processing

Raw RNA-sequencing data were obtained from the database of Genotypes and Phenotypes (dbGAP)-The Cancer Genome Atlas: phs000178; Genotype-Tissue Expression project: phs000424. RNA-sequencing reads were quantified to the human transcriptome (GENCODEv25) using Kallisto (v0.43.0) [22]. GENCODEv25 GTF was obtained from GENCODE [23], and a transcriptome fasta file was produced using the *rsem-prepare-reference* function of RSEM (version 1.2.26) [24]. Kallisto index was generated using the *kallisto index* function. Transcript level quantification was then obtained using the *kallisto quant* function. Gene level expression was obtained by summing the transcripts per million values for all transcripts within each gene. Student's *t* test was then used to compare expression in cancer and normal groups.

Statistical Analysis

All experiments were performed in duplicate or triplicate, and all data are expressed as the mean ± standard deviation. Statistical analysis was performed using GraphPad Prism version 6.00 for Windows (GraphPad Software). For single comparisons, an unpaired, two-tailed *t* test was used. For multiple comparisons, one-way analysis of variance (ANOVA) with Tukey's or Bonferroni post hoc test was performed. Results were considered statistically significant with a *P* value of less than or equal to .05. For all figures, $^{*}P < .05$, $^{**}P < .01$, $^{***}P < .001$, and $^{****}P < .0001$.

Results

Overexpression of DEK in Ovarian Cancer Cell Lines and Primary Ovarian Carcinomas

We first sought to determine if DEK is overexpressed in ovarian cancer. Protein lysates from noncancerous human ovarian surface epithelial cells (hOSE) and a panel of human HGSOC cell lines including HEY1, PEO4, PEO1, OVCAR3, OVCAR8, CAOV3, and COV362 were analyzed for DEK expression by immunoblotting (Figure 1*A*). Recombinant DEK was used as a positive control. All of the queried cell lines overexpressed DEK compared to hOSE. To determine if primary human epithelial ovarian cancer specimens also demonstrated elevated DEK levels, immunohistochemistry was performed on an ovarian cancer tissue microarray containing 108 normal ovarian tissue samples and 91 paired ovarian carcinoma tissue samples (representative samples, Figure 1*B*). The tissue microarray was scored blindly on a scale of 0-3, with 0 indicating no expression and 3 indicating intense, diffuse staining. The average IHC score for tumor specimens was statistically higher than that for normal ovarian tissue (1.94 vs 1.15, $P < .0001$). We then assessed correlations between DEK expression levels and clinical parameters for the patient specimens in our tissue microarray; analysis did not demonstrate any statistically significant correlations, potentially due to small sample size (data not shown). To further strengthen our analysis, we extended our query to publically available RNA-seq data and found elevated DEK transcripts in ovarian cancer specimens as compared to controls (Figure 1*C*).

Decreasing DEK levels in Ovarian Cancer Cells Slows Growth and Enhances Chemosensitivity

To determine the impact of DEK levels on ovarian cancer cell growth and response to chemotherapy, we modulated DEK expression using small interfering RNA (siRNA) and short hairpin RNA (shRNA) methodologies. CAOV3 and OVCAR8 cells were transfected with control siRNA (siControl) or DEK siRNA (siDEK) for 24 hours or with lentiviral particles expressing shControl or three separate DEK shRNA (shDEK) for 72 hours. Cell lysates were prepared, and DEK expression was analyzed by immunoblotting. Both siRNA and shRNA targeting DEK decreased DEK protein levels; shRNA methods resulted in greater reduction in DEK levels than siRNA methods across cell lines (Figure 2, *Ai*, *Bi*, and *Ci*). Following siRNA transfection or shRNA lentiviral infection, ovarian cancer cells were treated with chemotherapy for an additional 48 hours, and resultant cell viability was assessed. For siRNA-transfected mock-treated CAOV3 cells, DEK knockdown did not significantly decrease cell viability compared to mock-treated control. Furthermore, treatment with cisplatin or panobinostat did not have any additive effect, perhaps due to incomplete knockdown (Figure 2*Aii*). In the OVCAR8 cells, DEK knockdown with siRNA significantly reduced cell viability for mock-, cisplatin-, or panobinostat-treated cells, suggesting that OVCAR8 cells are more sensitive to these therapies than CAOV3 (Figure 2*Aii*). In CAOV3 cells transfected with shRNA constructs targeting DEK, shDEK1 failed to reduce cell viability, while shDEK2 and shDEK3 constructs resulted in significantly reduced cell viability in the absence of additional cytotoxic treatment. In the CAOV3 cells, no additional change in cell viability was observed when cells were treated with the indicated chemotherapies (Figure 2, *Bii* and *Cii*). In contrast, all shRNA constructs targeting DEK significantly reduced cell viability for mock-treated OVCAR8 and OVCAR3 samples (Figure 2, *Bii* and *Cii*). With the addition of doxorubicin, further reduction in

Figure 2. Decreasing DEK levels sensitizes ovarian cancer cell lines to chemotherapy. (Ai) OVCAR8 or CAOV3 ovarian cancer cells were transfected with siRNA targeting control sequence or siDEK for 24 hours. Immunoblotting was performed on cell lysates for DEK expression. (Aii) After OVCAR8 and CAOV3 cells were transfected with siControl or siDEK for 24 hours, cells were treated for an additional 48 hours with cisplatin or panobinostat and assessed for cell viability by MTT assay. Statistical analysis was performed by ANOVA with Tukey's post hoc test; $^{*}P < .05$, $^{**}P < .01$, $^{***}P < .001$, $^{****}P < .0001$ versus siControl. (Bi) CAOV3, OVCAR8, and OVCAR3 cells were infected with a lentivirus expressing a short hairpin RNA targeting a control sequence (shControl1) or DEK nt 1165-1185 (shDEK1). Immunoblotting was performed on cell lysates 72 hours after infection for DEK expression. (Bii) Twenty-four hours after infection with shControl1 or shDEK1, cells were treated with cisplatin, doxorubicin, or panobinostat for an additional 48 hours and assessed for cell viability using an MTT assay. Statistical analysis was performed by ANOVA with Tukey's post hoc test; $^{*}P < .05$, $^{**}P < .01$, $^{***}P < .001$, $^{****}P < .0001$ versus shControl1. (Ci) Immunoblotting was performed on cell lysates following infection with lentiviral constructs with shControl2, shDEK2 (nt 860-880), or shDEK3 (nt 1192-1216). (Cii) Twenty-four-hour infection with shControl2, shDEK2, or shDEK3 followed by treatment with indicated therapies. Statistical analysis was performed by ANOVA with Tukey's post hoc test; $^{*}P < .05$, $^{**}P < .01$, $^{***}P < .001$, $^{****}P < .0001$ versus shControl2. (Di) Following lentiviral infection with shControl1 or shDEK1, stable polyclonal cell lines were generated after selection with 0.25 μg/ml of puromycin. Growth curves were generated by counting total number of cells every 24 hours for 6 days. Statistical analysis was performed by ANOVA with Bonferroni post hoc test. $^{**}P < .01$, $^{***}P < .001$, $^{****}P < .0001$ versus shControl1. (Dii) Growth curves were generated in stable lines expressing shControl2, shDEK2, or shDEK. Statistical analysis was performed by ANOVA with Bonferroni post-hoc test. $^{**}P < .01$,$^{***}P < .001$, $^{****}P < .0001$ versus shControl2.

cell viability was consistently observed for both OVCAR8 and OVCAR3 cells. Cisplatin only reduced cell viability in the OVCAR3 cells infected with shDEK2 or shDEK3 constructs, and treatment with panobinostat reduced viability in the OVCAR8 cells for shDEK1 and shDEK2 and OVCAR3 infected with shDEK1 (Figure 2 *Bii* and *Cii*). Overall, these results suggest that DEK expression is important for cell viability and chemotherapy resistance, but the impact of decreasing DEK levels on cellular function may depend on specific cancer cell characteristics. The level of DEK expression likely impacts phenotype, as DEK depletion was not as complete in the CAOV3 cells, which show fewer phenotypic effects following shDEK infection.

Given our finding that decreasing DEK levels in ovarian cancer cells with shRNA methods results in decreased cell viability, we sought to determine if decreased DEK expression affected ovarian

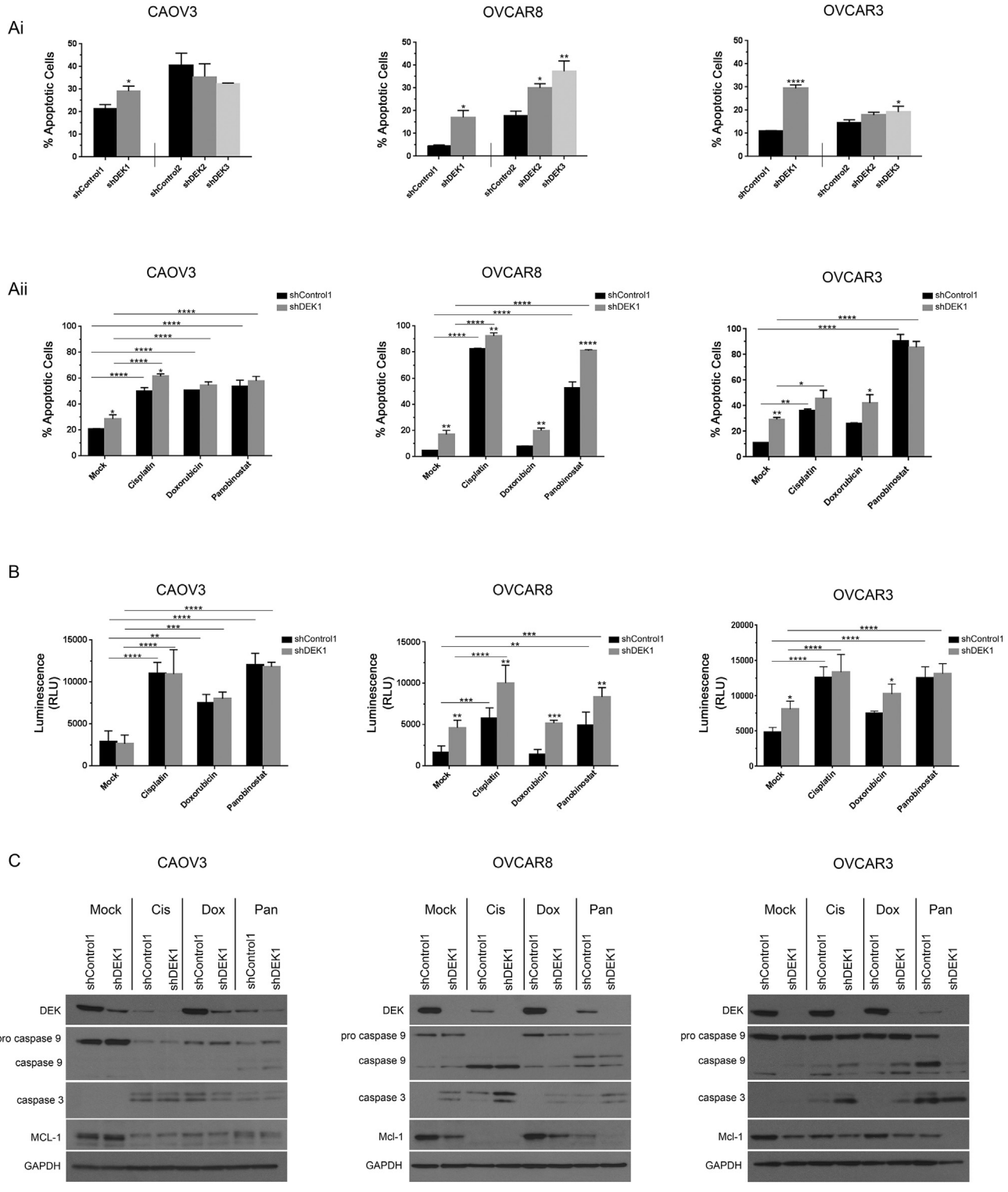

cancer cell growth rates. Polyclonal stable cell lines expressing control or DEK targeting shRNAs were generated in CAOV3, OVCAR8, and OVCAR3 cells (Figure 2, *Di* and *Dii*). Each cell line was assessed for growth every 24 hours over 6 days. In all three cell lines, decreased DEK levels resulted in significantly reduced cell growth, indicating that DEK plays a role in cell proliferation (Figure 2, *Di* and *Dii*).

Decreased DEK Levels Promote Apoptotic Cell Death

We next assessed the impact of decreasing DEK levels on the induction of ovarian cancer apoptotic cell death. Cell lines were infected with shControl or shDEK for 24 hours followed by treatment with cisplatin, doxorubicin, or panobinostat for 48 hours. Apoptosis was first evaluated by Annexin-V and propidium iodide staining via flow cytometric analysis (Figure 3, *Ai* and *Aii*). In CAOV3 cells, neither decreased DEK levels nor chemotherapy treatment in addition to DEK knockdown significantly induced cellular apoptosis when compared to shControl treated samples (Figure 3, *Ai* and *Aii*). However, a significant increase in apoptotic cells was observed following shRNA-mediated decrease in DEK levels in OVCAR8 and OVCAR3 cells following infection with all shDEK constructs (Figure 3*Ai*). Furthermore, the addition of a chemotherapeutic agent augmented this effect, as demonstrated by a significantly higher percentage of apoptotic cells following concurrent treatment with cisplatin, doxorubicin, or panobinostat in the OVCAR8 cells. Only doxorubicin increased apoptosis in the OVCAR3 cells (Figure 3*Aii*). Apoptosis was also assessed by cleaved caspase-3/7 luminescence assay. CAOV3 cells did not demonstrate increased cleaved caspase-3/7 activity in any of the tested treatment conditions (Figure 3*B*). In contrast, OVCAR3 cells demonstrated increased cleaved caspase-3/7 activity for mock and doxorubicin treatment conditions. OVCAR8 cells showed increased cleaved caspase-3/7 activity for all treatment conditions, with shDEK cells treated with cisplatin and panobinostat resulting in the highest cleavage of caspase-3/7 (Figure 3*B*).

To confirm an apoptotic mechanism of cell death, Western blot analysis was performed on cell lysates following reduction of DEK levels in ovarian cancer cell lines. In OVCAR8 and OVCAR3 cells, increased expression of cleaved caspase-9 and cleaved caspase-3 was observed for shDEK infected cells, and treatment with chemotherapeutic agents increased expression compared to shControl infected cell (Figure 3*C*). In all DEK-depleted conditions for OVCAR8 and OVCAR3 cells, MCL-1 expression was diminished compared to shControl infected cells. Furthermore, reduced levels of MCL-1 were observed after cisplatin, doxorubicin, and panobinostat treatment in OVCAR8 and OVCAR3 cells, suggesting DEK mediates MCL-1 expression in ovarian cancer. To confirm these findings, immunoblot signal intensity for caspase-9, caspase-3, and MCL-1 was quantified (Supplementary Figure 1). These results indicate that decreased DEK expression promotes apoptosis through caspase cleavage and the reduction of MCL-1 expression.

Decreased DEK Levels Result in Increased DNA Double-Strand Breaks

We next assessed the role of decreasing DEK levels on DNA damage. CAOV3, OVCAR8, or OVCAR3 cells were infected with control or DEK targeting shRNAs for 24 hours followed by treatment with the indicated concentrations of cisplatin, doxorubicin, or panobinostat for an additional 24 hours. Immunoblotting was performed to evaluate the phosphorylation of γH2A, a histone phosphorylated in response to double-strand DNA breaks, and levels of Rad51, a protein specific to the homologous recombination pathway. Results were noted to be dependent on the specific cell line. In CAOV3 cells, decreasing DEK levels did not alter γH2A phosphorylation or Rad51 expression following treatment with cisplatin or panobinostat; however, increased γH2A phosphorylation and increased Rad51 expression were noted when cells were infected with shDEK2 and shDEK3 constructs and treated with doxorubicin (Figure 4, *A* and *B*). In contrast, cisplatin or panobinostat treatment of OVCAR8 and OVCAR3 cells resulted in the highest levels of phosphorylated γH2A. In OVCAR3 cells, decreased DEK levels in the absence of concurrent chemotherapy increased DNA double-strand breaks as detected by increased levels of phosphorylated γH2A. Interestingly, Rad51 expression decreased under some treatment conditions and was lower in DEK-deficient OVCAR8 cells treated with concurrent chemotherapy. Decreased Rad51 levels following panobinostat therapy has also been reported in other tumor types [25]. We conclude from these findings that both cisplatin and panobinostat treatments result in marked cellular toxicity and DNA damage for both shControl and shDEK, while the more modest effects of doxorubicin alone trended toward increased sensitivity to the effects of reduced DEK levels.

To further characterize DNA damage following modulation of DEK levels and treatment with chemotherapy, immunofluorescence was performed to detect phosphorylated γH2A foci (Supplementary Figure 2). In CAOV3 and OVCAR8 cells, phosphorylated γH2A immunofluorescence was not altered with decreased DEK expression, while cisplatin treatment resulted in the highest level of γH2A foci for both cell lines. In contrast, decreasing DEK expression in the

Figure 3. Decreasing DEK levels in ovarian cancer cell lines induces apoptosis that is enhanced with concurrent chemotherapy. (Ai) CAOV3, OVCAR8, or OVCAR3 cells were infected with lentivirus expressing shControl1 or shDEK1 mock treated or shControl2, shDEK2, or shDEK3 mock treated for 72 hours. Cells were harvested and incubated with Annexin V-FITC and propidium iodide followed by assessment with flow cytometry. Annexin V–positive cells were characterized as apoptotic. Statistical analysis was performed by Student's *t* test or ANOVA with Bonferroni post hoc test; $^{*}P < .05$, $^{**}P < .01$, $^{***}P < .001$, $^{****}P < .0001$ versus shControl1 or shControl2. (Aii) Cells were infected with shControl1 or shDEK1 for 24 hours followed by treatment with cisplatin, doxorubicin, or panobinostat for an additional 48 hours. Following treatment, cells were harvested and incubated with Annexin V-FITC and propidium iodide, and flow cytometry was performed Statistical analysis was performed by ANOVA with Tukey's post hoc test.; $^{*}P < .05$, $^{**}P < .01$, $^{***}P < .001$, $^{****}P < .0001$ versus shControl1. Total apoptotic cells in each sample were normalized to shControl-infected cells. (B) Levels of cleaved caspases 3/7 were detected by a luminescence assay in cells treated infected with shControl or shDEK1 for 24 hours followed by treatment with indicated concentrations of cisplatin, doxorubicin, or panobinostat for 48 hours. Statistical analysis was performed by ANOVA with Tukey's post hoc test.;$^{*}P < .05$, $^{**}P < .01$, $^{***}P < .001$, $^{****}P < .0001$ versus shControl1. (C) Following infection with shControl1 or shDEK1 for 24 hours, cells were treated for an additional 48 hours with cisplatin, doxorubicin, or panobinostat; cells were lysed; and samples containing equal amount of protein were analyzed by immunoblotting using indicated antibodies.

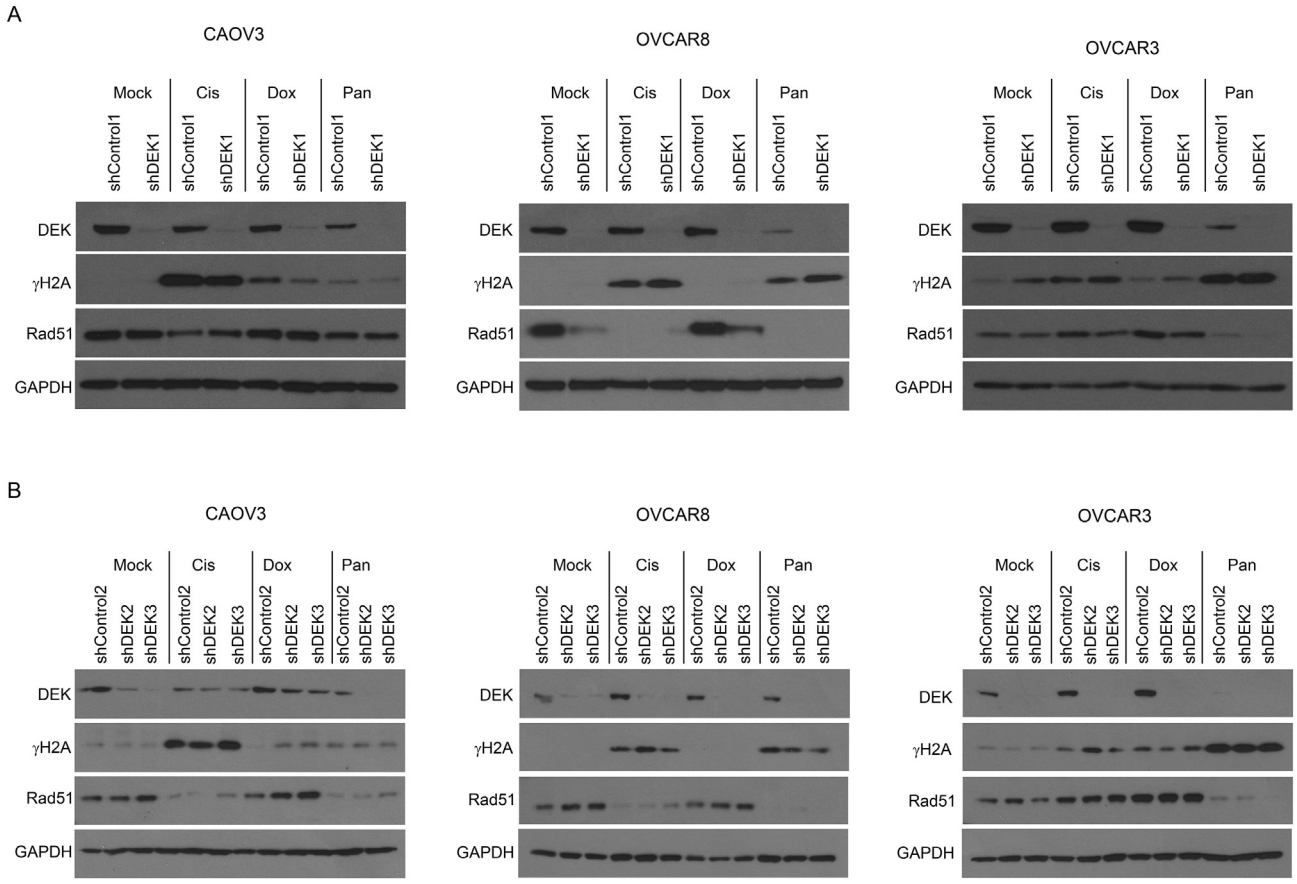

Figure 4. Decreasing DEK levels increases DNA damage. (A) CAOV3, OVCAR8, or OVCAR3 cells were infected with lentivirus expressing shControl1 or shDEK1. Twenty-four hours after infection, cells were treated with cisplatin, doxorubicin, or panobinostat for an additional 24 hours. Cells were harvested, and equal amounts of protein were immunoblotted for DEK, phosphorylated serine 139 on histone γH2A, Rad51, and GAPDH. (B) Ovarian cancer cell lines were infected with lentivirus expressing shControl2, shDEK2, or shDEK3 for 24 hours and then treated with indicated therapies for an additional 24 hours, followed by preparation of lysates and immunoblotting for phosphorylated serine 139 on histone γH2A, Rad51, and GAPDH.

OVCAR3 cells with concurrent treatment trended toward increased DNA double-strand breaks as indicated by increased number of γH2A foci, and cisplatin treatment significantly increased the number of foci per cell (Supplementary Figure 2). Together, these results suggest that decreased DEK expression with concurrent chemotherapeutic treatment promotes DNA double-strand breaks in a cell line–dependent manner.

Decreased DEK Levels Slow Ovarian Cancer Xenograft Growth In Vivo

Finally, using a mouse xenograft model, we sought to determine if modulating DEK levels alters tumor growth *in vivo*. Polyclonal CAOV3 cells (500,000) with stable expression of either control or DEK-targeting shRNA were injected into NOD-SCID mice, and tumor growth was monitored. Tumors expressing DEK-targeting shRNA grew significantly slower than control tumors (Figure 5*A*). Following animal sacrifice, primary tumors were isolated and weighed. Tumors isolated from mice injected with control shRNA expressing cells were significantly larger than those isolated from mice injected with DEK-targeting shRNA (Figure 5*B*). Immunohistochemical analysis indicated that DEK expression was undetectable in tumors isolated from mice injected with cells expressing DEK-targeting shRNA (Figure 5*C*). It is of note that these striking *in vivo* results were obtained using the CAOV3 cell line that is least sensitive to apoptosis following DEK depletion *in vitro* (Figure 3, *Ai*, *B*, and *C*). Due to the dramatic difference in tumor growth and significantly smaller tumors following decreased DEK levels, concurrent chemotherapy treatment in the xenograft model system failed to demonstrate further reduction in tumor growth (data not shown).

Discussion

Herein we show that HGSOC primary tumors and cell lines demonstrate elevated levels of the DEK oncoprotein. Decreasing DEK levels in ovarian cancer cell lines promotes apoptotic cell death. We find that decreasing DEK levels reduced MCL-1 expression, consistent with findings in melanoma, where decreasing DEK levels leads to greater sensitivity to the doxorubicin-induced apoptosis that is mediated by MCL-1 [18]. Notably, we demonstrate the critical new unique finding of this study that, in some HGSOCs, decreasing DEK levels is sufficient to induce cell death even in the absence of concurrent chemotherapy.

We find that the response to decreased DEK levels varies by cell line. CAOV3 cells, for instance, demonstrate a relative resistance to both decreasing DEK levels and chemotherapy. In contrast, both OVCAR3 and OVCAR8 are more sensitive to decreased DEK levels, resulting in decreased cell viability and increased apoptosis. This variability in effects may be due at least in part to the range of DEK depletion in the various cell lines and with different methodologies of

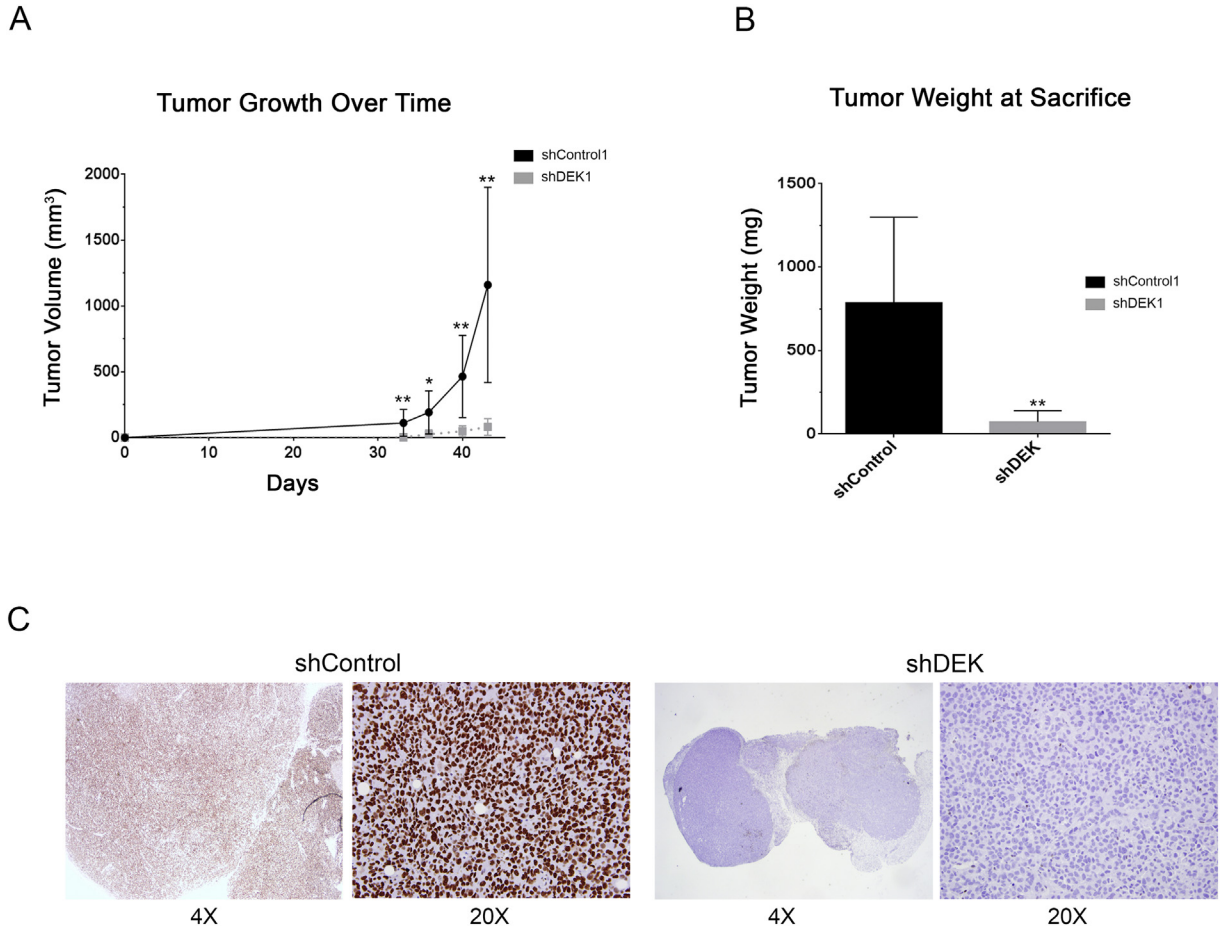

Figure 5. Decreasing DEK levels slows ovarian cancer xenograft growth. Mice were injected with 5×10^5 CAOV3 cells stably expressing short hairpin RNAs targeting control sequences or DEK nt1165-1185 in bilateral axillae. (A) Once tumors were palpable, tumor sizes were measured weekly until the total tumor burden reached 2000 mm^3. (B). Upon animal sacrifice, tumors were weighed. (C) DEK immunohistochemistry was performed on tumors to demonstrate DEK knockdown. Statistical analysis in A and B was performed using a Student's *t* test, shControl versus shDEK $^*P < .05$, $^{**}P < .01$, $^{***}P < .001$.

siRNA versus shRNA (Figure 2, *Ai* and *Bi*). Consistent with HGSOC histology, all three of these lines harbor p53 mutation; however, the variability in effects may be due to additional genetic and/or epigenetic cellular changes. Additional genetic alterations may underlie the phenotypic characteristics demonstrated in our study, and this remains an area for future study. The complex nature of the role of DEK in the pathogenesis of different ovarian cancers is illustrated by the striking reduction in tumor growth *in vivo* when DEK expression is reduced in CAOV3, a cell line whose degree of apoptosis and DNA damage is minimally affected by DEK knockdown *in vitro*. The range in effects both across cell lines and in different experimental systems highlights the potential challenge in identifying the best patient population in whom to ultimately develop DEK-based therapeutic strategies. To this end, we continue to expand our studies of the role of DEK in ovarian cancer both across a broader panel of ovarian cancer cell lines and in primary patient-derived specimens, with the goal of determining predictive biomarkers of a favorable antitumor response to decreasing DEK levels.

The finding that decreasing DEK levels results in slowed tumor growth in animal model xenografts suggests a potential therapeutic strategy for treating patients. One of the challenges in efforts to exploit DEK as a therapeutic target in HGSOC is that DEK is a structural protein with no identified enzymatic activity. Thus, development of a small molecule inhibitor of an enzymatic domain is not possible, and continued studies are under way to determine critical effectors of the phenotype observed herein to define a potential therapeutic approach. We recently developed a single-stranded DNA aptamer that greatly attenuates DEK activity *in vivo* [26], and intracellular delivery of this agent could potentially prove useful in the treatment of ovarian cancer. Additionally, decreasing DEK levels may serve as a model of altering cellular DNA damage repair pathways to shift both cell growth properties and response to standard chemotherapeutic agents.

In the setting of recurrent ovarian cancer, clinical decisions regarding the next chemotherapeutic agent are often predicated on "platinum sensitivity." Patients with a disease-free interval of greater than 6 months are considered platinum-sensitive and are treated with a platinum-based regimen, while those with a disease-free interval of less than 6 months are termed platinum-resistant and receive nonplatinum therapies. One of the fundamental challenges in the treatment of epithelial ovarian cancer is the development of platinum resistance. The field of ovarian cancer treatment is undergoing a rapid shift with the development of predictors of response to therapy. Specifically, the presence of homologous recombination deficiency is predictive of platinum sensitivity, and an increasing number of tests are becoming clinically available to help guide treatment decisions. DEK overexpression in patient tumors may serve as a biomarker of resistance to

conventional chemotherapy. Although recent work demonstrates that DEK functions in DNA damage repair via HR in addition to nonhomologous end-joining [9], further work is necessary to define the specific DNA damage repair functions of DEK in ovarian cancer. It is likely that ultimately tumors will undergo assessment of both HR and nonhomologous end-joining with the classification of DNA damage repair pathway status influencing treatment strategies.

Conclusions

DEK is overexpressed in HGSOCs, and decreasing DEK levels significantly reduces cell viability and tumor growth, resulting in apoptotic cell death. Given the critical need for new treatment strategies for ovarian cancer, these findings highlight an exciting new pathway with therapeutic potential.

Supplementary data to this article can be found online at https://doi.org/10.1016/j.neo.2018.10.005.

Acknowledgements

The authors would like to acknowledge technical assistance provided by Penny Yang.

References

[1] Ferlay J, Soerjomataram I, Dikshit R, Eser S, Mathers C, Rebelo M, Parkin DM, Forman D, and Bray F (2015). Cancer incidence and mortality worldwide: sources, methods and major patterns in GLOBOCAN 2012. *Int J Cancer* **136** (5), E359-386. https://dx.doi.org/10.1002/ijc.29210 [Epub 2014/09/16. PubMed PMID: 25220842].

[2] Siegel RL, Miller KD, and Jemal A (2017). Cancer statistics, 2017. *CA Cancer J Clin* **67**(1), 7–30. https://dx.doi.org/10.3322/caac.21387 [Epub 2017/01/06. PubMed PMID: 28055103].

[3] Konstantinopoulos PA, Ceccaldi R, Shapiro GI, and D'Andrea AD (2015). Homologous recombination deficiency: exploiting the fundamental vulnerability of ovarian cancer. *Cancer Discov* **5**(11), 1137–1154. https://dx.doi.org/10.1158/2159-8290.CD-15-0714 [PubMed PMID: 26463832; PMCID: 4631624].

[4] Ledermann JA, Drew Y, and Kristeleit RS (2016). Homologous recombination deficiency and ovarian cancer. *Eur J Cancer* **60**, 49–58. https://dx.doi.org/10.1016/j.ejca.2016.03.005 [PubMed PMID: 27065456].

[5] Cancer Genome Atlas Research N (2011). Integrated genomic analyses of ovarian carcinoma. *Nature* **474**(7353), 609–615. https://dx.doi.org/10.1038/nature10166 [PubMed PMID: 21720365; PMCID: 3163504].

[6] Bast Jr RC, Hennessy B, and Mills GB (2009). The biology of ovarian cancer: new opportunities for translation. *Nat Rev Cancer* **9**(6), 415–428. https://dx.doi.org/10.1038/nrc2644 [Epub 2009/05/23. PubMed PMID: 19461667; PMCID: PMC2814299].

[7] Bolton KL, Chenevix-Trench G, Goh C, Sadetzki S, Ramus SJ, Karlan BY, Lambrechts D, Despierre E, Barrowdale D, and McGuffog L, et al (2012). Association between BRCA1 and BRCA2 mutations and survival in women with invasive epithelial ovarian cancer. *JAMA* **307**(4), 382–390. https://dx.doi.org/10.1001/jama.2012.20 [PubMed PMID: 22274685; PMCID: PMC3727895].

[8] Kavanaugh GM, Wise-Draper TM, Morreale RJ, Morrison MA, Gole B, Schwemberger S, Tichy ED, Lu L, Babcock GF, and Wells JM, et al (2011). The human DEK oncogene regulates DNA damage response signaling and repair. *Nucleic Acids Res* **39**(17), 7465–7476. https://dx.doi.org/10.1093/nar/gkr454 [PubMed PMID: 21653549; PMCID: 3177200].

[9] Smith EA, Gole B, Willis NA, Soria R, Starnes LM, Krumpelbeck EF, Jegga AG, Ali AM, Guo H, and Meetei AR, et al (2017). DEK is required for homologous recombination repair of DNA breaks. *Sci Rep* **7**, 44662. https://dx.doi.org/10.1038/srep44662 [Epub 2017/03/21. PubMed PMID: 28317934].

[10] Alexiadis V, Waldmann T, Andersen J, Mann M, Knippers R, and Gruss C (2000). The protein encoded by the proto-oncogene DEK changes the topology of chromatin and reduces the efficiency of DNA replication in a chromatin-specific manner. *Genes Dev* **14**(11), 1308–1312 [Epub 2000/06/03. PubMed PMID: 10837023; PMCID: PMC316669].

[11] Deutzmann A, Ganz M, Schonenberger F, Vervoorts J, Kappes F, and Ferrando-May E (2015). The human oncoprotein and chromatin architectural factor DEK counteracts DNA replication stress. *Oncogene* **34**(32), 4270–4277. https://dx.doi.org/10.1038/onc.2014.346 [PubMed PMID: 25347734].

[12] Sammons M, Wan SS, Vogel NL, Mientjes EJ, Grosveld G, and Ashburner BP (2006). Negative regulation of the RelA/p65 transactivation function by the product of the DEK proto-oncogene. *J Biol Chem* **281**(37), 26802–26812. https://dx.doi.org/10.1074/jbc.M600915200 [PubMed PMID: 16829531].

[13] McGarvey T, Rosonina E, McCracken S, Li Q, Arnaout R, Mientjes E, Nickerson JA, Awrey D, Greenblatt J, and Grosveld G, et al (2000). The acute myeloid leukemia-associated protein, DEK, forms a splicing-dependent interaction with exon-product complexes. *J Cell Biol* **150**(2), 309–320 [Epub 2000/07/26. PubMed PMID: 10908574; PMCID: PMC2180225].

[14] Privette Vinnedge LM, McClaine R, Wagh PK, Wikenheiser-Brokamp KA, Waltz SE, and Wells SI (2011). The human DEK oncogene stimulates beta-catenin signaling, invasion and mammosphere formation in breast cancer. *Oncogene* **30**(24), 2741–2752. https://dx.doi.org/10.1038/onc.2011.2 [Epub 2011/02/15. PubMed PMID: 21317931; PMCID: PMC3117026].

[15] Hua Y, Hu H, and Peng X (2009). Progress in studies on the DEK protein and its involvement in cellular apoptosis. *Sci China C Life Sci* **52**(7), 637–642. https://dx.doi.org/10.1007/s11427-009-0088-2.

[16] Kim DW, Chae JI, Kim JY, Pak JH, Koo DB, Bahk YY, and Seo SB (2009). Proteomic analysis of apoptosis related proteins regulated by proto-oncogene protein DEK. *J Cell Biochem* **106**(6), 1048–1059. https://dx.doi.org/10.1002/jcb.22083 [PubMed PMID: 19229864].

[17] Lee KS, Kim DW, Kim JY, Choo JK, Yu K, and Seo SB (2008). Caspase-dependent apoptosis induction by targeted expression of DEK in Drosophila involves histone acetylation inhibition. *J Cell Biochem* **103**(4), 1283–1293. https://dx.doi.org/10.1002/jcb.21511 [PubMed PMID: 17685435].

[18] Khodadoust MS, Verhaegen M, Kappes F, Riveiro-Falkenbach E, Cigudosa JC, Kim DS, Chinnaiyan AM, Markovitz DM, and Soengas MS (2009). Melanoma proliferation and chemoresistance controlled by the DEK oncogene. *Cancer Res* **69**(16), 6405–6413. https://dx.doi.org/10.1158/0008-5472.CAN-09-1063 [PubMed PMID: 19679545; PMCID: 2727675].

[19] Kappes F, Waldmann T, Mathew V, Yu J, Zhang L, Khodadoust MS, Chinnaiyan AM, Luger K, Erhardt S, and Schneider R, et al (2011). The DEK oncoprotein is a Su(var) that is essential to heterochromatin integrity. *Genes Dev* **25**(7), 673–678. https://dx.doi.org/10.1101/gad.2036411 [Epub 2011/04/05. PubMed PMID: 21460035; PMCID: 3070930].

[20] Privette Vinnedge LM, Benight NM, Wagh PK, Pease NA, Nashu MA, Serrano-Lopez J, Adams AK, Cancelas JA, Waltz SE, and Wells SI (2015). The DEK oncogene promotes cellular proliferation through paracrine Wnt signaling in Ron receptor-positive breast cancers. *Oncogene* **34**(18), 2325–2336. https://dx.doi.org/10.1038/onc.2014.173 [Epub 2014/06/24. PubMed PMID: 24954505; PMCID: PMC4275425].

[21] Kononen J, Bubendorf L, Kallioniemi A, Barlund M, Schraml P, Leighton S, Torhorst J, Mihatsch MJ, Sauter G, and Kallioniemi OP (1998). Tissue microarrays for high-throughput molecular profiling of tumor specimens. *Nat Med* **4**(7), 844–847 [Epub 1998/07/14. PubMed PMID: 9662379].

[22] Bray NL, Pimentel H, Melsted P, and Pachter L (2016). Near-optimal probabilistic RNA-seq quantification. *Nat Biotechnol* **34**(5), 525–527. https://dx.doi.org/10.1038/nbt.3519 [PubMed PMID: 27043002].

[23] Harrow J, Frankish A, Gonzalez JM, Tapanari E, Diekhans M, Kokocinski F, Aken BL, Barrell D, Zadissa A, and Searle S, et al (2012). GENCODE: the reference human genome annotation for The ENCODE Project. *Genome Res* **22** (9), 1760–1774. https://dx.doi.org/10.1101/gr.135350.111 [PubMed PMID: 22955987; PMCID: PMC3431492].

[24] Li B and Dewey CN (2011). RSEM: accurate transcript quantification from RNA-Seq data with or without a reference genome. *BMC Bioinformatics* **12**, 323. https://dx.doi.org/10.1186/1471-2105-12-323 [PubMed PMID: 21816040; PMCID: PMC3163565].

[25] Xie C, Drenberg C, Edwards H, Caldwell JT, Chen W, Inaba H, Xu X, Buck SA, Taub JW, and Baker SD, et al (2013). Panobinostat enhances cytarabine and daunorubicin sensitivities in AML cells through suppressing the expression of BRCA1, CHK1, and Rad51. *PLoS One* **8**(11)e79106. https://dx.doi.org/10.1371/journal.pone.0079106 [Epub 2013/11/19. PubMed PMID: 24244429; PMCID: PMC3823972].

[26] Mor-Vaknin N, Saha A, Legendre M, Carmona-Rivera C, Amin MA, Rabquer BJ, Gonzales-Hernandez MJ, Jorns J, Mohan S, and Yalavarthi S, et al (2017). DEK-targeting DNA aptamers as therapeutics for inflammatory arthritis. *Nat Commun* **8**, 14252. https://dx.doi.org/10.1038/ncomms14252 [Epub 2017/02/07. PubMed PMID: 28165452].